

## A bevy of area-preserving transforms for map projection designers

Daniel “daan” Strebe

To cite this article: Daniel “daan” Strebe (2018): A bevy of area-preserving transforms for map projection designers, *Cartography and Geographic Information Science*, DOI: [10.1080/15230406.2018.1452632](https://doi.org/10.1080/15230406.2018.1452632)

To link to this article: <https://doi.org/10.1080/15230406.2018.1452632>



Published online: 05 Apr 2018.



Submit your article to this journal [↗](#)




View related articles [↗](#)



View Crossmark data [↗](#)



# A bevy of area-preserving transforms for map projection designers

Daniel “daan” Strebe 

Mapmathematics LLC, Seattle, WA, USA

## ABSTRACT

Sometimes map projection designers need to create equal-area projections to best fill the projections' purposes. However, unlike for conformal projections, few transformations have been described that can be applied to equal-area projections to develop new equal-area projections. Here, I survey area-preserving transformations, giving examples of their applications and proposing an efficient way of deploying an equal-area system for raster-based Web mapping. Together, these transformations provide a toolbox for the map projection designer working in the area-preserving domain.

## ARTICLE HISTORY

Received 1 January 2018  
Accepted 12 March 2018

## KEYWORDS

Map projection; equal-area projection; area-preserving transformation; area-preserving homotopy; Strebe 1995 projection

## 1. Introduction

It is easy to construct a new conformal projection: Find an existing conformal projection and apply any complex analytic function to it. Voilà, new conformal projection! In practice, finding the right function for the purpose usually takes some work, but nevertheless, the toolbox is rich and powerful. Not so for equal-area projections. A few techniques have been exploited over the centuries, even fewer explicitly described, and in general the domain remains lightly explored. No area-preserving analog to complex analysis is known to exist.

This work doesn't solve such big problems. Instead, it collects together in one place a body of techniques map projection designers can use to efficiently generate new equal area map projections. Some are obvious; some are simple but clever; some are a little more involved. Their inventions range from centuries ago to being introduced in this paper. I give examples with particular attention to a novel replacement scheme for the Web Mercator.

Since the advent of digital computers, several iterative methods for minimizing distortion across a chosen region have appeared in the literature. Iterative systems are specifically outside the purview of this work. They are adequately described by their authors in any case. I invite the interested reader to peruse, for example, Dyer and Snyder (1989) or Canters (2002, pp. 115–244).

For simplicity, I discuss the manifold to be projected as a sphere, but the techniques I describe generally do not depend on this specificity. The techniques fall into

two categories: plane-to-plane transformations and “sphere-to-sphere” transformations – but in quotes because the manifold need not be a sphere at all. Some of the techniques combine both kinds of transformations or use the plane as an intermediary.

In the case of plane-to-plane transformations, the presumption is that the manifold has been projected to the plane already in a way that preserves areas. Hence, the consideration is purely planar, and regardless of what manifold was designated as the original surface before projecting, the only question is whether the plane-to-plane transformation itself preserves area measure.

### 1.1. Terminology

Terminology is not well standardized for equal-area projections. More in line with the field of differential geometry than with mathematical cartography, the title of this paper uses the term *area-preserving transformation* so as to be readily understandable to the widest audience. However, I do not use that term in the body of this text. To avoid the awkwardness of noun forms of *equal-area*, I will sometimes use *equivalence*. The term *authalic* also appears in the literature, but is redundant to my needs here and will not be used.

### 1.2. Symbols

- $\lambda$  refers to a geodetic longitude;
- $\varphi$  refers to a geodetic latitude;

- $\theta$  refers to a counterclockwise angle from positive  $x$  axis on the cartesian plane;
- $\rho$  refers to a distance from origin on the cartesian plane;
- ' added to a variable name denotes a variable transformed from the variable of the same name that lacks the prime symbol.

## 2. Transformations

### 2.1. Scaling

As noted by Strebe (2016), the equal-area property for a mapping from sphere to plane can be defined either strictly or loosely: strictly in that

$$\frac{\partial y}{\partial \varphi} \frac{\partial x}{\partial \lambda} - \frac{\partial y}{\partial \lambda} \frac{\partial x}{\partial \varphi} = R^2 \cos \varphi, \quad (2.1)$$

(with  $R$  being the radius of the generating globe) or loosely in that

$$\frac{\partial y}{\partial \varphi} \frac{\partial x}{\partial \lambda} - \frac{\partial y}{\partial \lambda} \frac{\partial x}{\partial \varphi} = s \cos \varphi, \quad (2.2)$$

with  $s$  being any non-zero, finite, real value. The rationale for the strict case is that the projection maps regions on the globe to the regions on the plane such that the area measure of any mapped region remains the same as the area measure of the unmapped region. The rationale for the looser case is that relative areas are preserved throughout the map, regardless of how their area measure might be scaled with respect to the generating globe. Simple, isotropic scaling is an area-preserving transformation by the looser condition.

On its own, scaling is not terribly interesting. Combined with other techniques, however, it becomes powerful, as we shall see in subsequent sections.

### 2.2. Affine transformation

Also noted by Strebe (2016), affine transformation preserves areas. That is, given  $x$  and  $y$  as the planar coordinates of an equal-area map projection,

$$\begin{bmatrix} a & b \\ c & d \end{bmatrix} \begin{bmatrix} x \\ y \end{bmatrix} = \begin{bmatrix} x' \\ y' \end{bmatrix} \quad (2.3)$$

$x', y'$  is also equal-area, provided the matrix is not singular and  $a, b, c, d$  are constant. When  $b = 0, c = 0, a = d$ , the affine transformation degenerates to the simple, isotropic scaling described in Section 2.1. With  $b = 0, c = 0, a \neq d$ , the affine transformation describes a scaling such that the  $x$  and  $y$  directions scale differently. This can be useful, particularly when  $d = 1/a$ . This last case preserves overall area

of the map, and can adjust the proportions and distortion characteristics of the map to better suit the purpose. A common example is based on the cylindric equal-area presented by Lambert (Tobler, 1972), with primitive formulae

$$L_{cea} = \begin{bmatrix} x & = \lambda \\ y & = \sin(\varphi) \end{bmatrix}. \quad (2.4)$$

In its original form, the projection has no distortion along the equator, and “correct” scale there. By scaling the height by  $\sec \varphi_0$  and the width by  $\cos \varphi_0$ , a chosen latitude  $\varphi_0$  can be made to have no distortion and to represent nominal scale. No less than seven variants of Lambert’s original that use this technique have been formally described independently by nine others, including:

- Gall (1885) ( $\varphi_0 = 45^\circ$ , “Gall orthographic,” now usually “Gall–Peters,” presented in 1855)
- Smyth (1870) ( $\varphi_0 = \arccos \sqrt{2/\pi}$ , “Smyth’s equal-surface”)
- Behrmann (1910) ( $\varphi_0 = 30^\circ$ )
- Craster (1929) (identical to Smyth equal-surface)
- Balthasart (1935) ( $\varphi_0 = 50^\circ$ )
- Edwards (1953) ( $\varphi_0 = 37^\circ 24'$ , “Trystan Edwards”)
- Peters (1983) (identical to Gall orthographic, first public mention in 1967)
- Tobler and Chen (1986) ( $\varphi_0 = \arccos \sqrt{1/\pi}$ , “Tobler’s world in a square”)
- Abramms (2006) ( $\varphi_0 = 37^\circ 30'$ , “Hobo–Dyer,” commissioned in 2002)

Each of these projections can be described as an affine transformation on Lambert’s cylindric equal-area:

$$\begin{bmatrix} \cos \varphi_0 & 0 \\ 0 & \sec \varphi_0 \end{bmatrix} \cdot L_{cea}. \quad (2.5)$$

Other examples of this technique can be found in pseudocylindric projections when the simplest form of the generating formulae does not yield the desired latitude to be free of distortion along the central meridian. Boggs (1929), for example, stretches  $x$  to slightly more than twice the primitive formulae’s results, and compresses  $y$  by the reciprocal.

Affine transformation relates to the scaling constant  $s$  reported in Equation (2.2). Letting

$$A = \begin{bmatrix} a & b \\ c & d \end{bmatrix} \quad (2.6)$$

such that  $A$  is not singular and  $a, b, c, d$  are constant when applying  $A$  to the projection, then

$$s = \det A, \quad (2.7)$$

with  $\det$  being the determinant.

I found no instance of affine transformation with shear components exploited in cartographic maps before Strebe (2017). As will be seen in Section 2.9, general affine transformations can serve useful purposes in conjunction with other transformations. However, perhaps the value of affine transformation on its own has been underappreciated, as discussed next.

Consider an arbitrary, non-conformal projection  $P$ . As described by Tissot (1881), the distortion undergone by a geographical point  $p$  when projected by  $P$  can be described as the projection of an infinitesimal circle around  $p$  into an infinitesimal ellipse on the plane. The area of this projected *Tissot ellipse*, as a ratio to the original circle from the sphere, gives the amount of *flation* (or, areal inflation or deflation, as per Battersby, Strebe, and Finn (2017)) at the projected point.

Angles also undergo changes when projected. Anchored at the center of the unprojected circle, we can construct an unlimited number of orthogonal axes, each rotated from the rest. When projecting, there will always be some orthogonal axis from the sphere that remains orthogonal on the plane and therefore remains undeformed. Conversely, some axis originally orthogonal must undergo greater deformation than any other when projected. Likewise, axes will exist for every angle in between undeformed and maximally deformed. It is the greatest deformation that is used to characterize angular deformation at the point. The ratio of the major and minor axes of the Tissot ellipse can be used to compute that maximal angular deformation.

Laskowski (1989) describes the relationship of a projection's Jacobian matrix  $J$  to the projection's local distortion:

$$T = J \cdot \begin{bmatrix} N \cos \varphi & 0 \\ 0 & M \end{bmatrix}^{-1} \quad (2.8)$$

where  $N$  is the meridional radius of curvature and  $M$  is the radius of curvature for the parallel. For the sphere, both  $N$  and  $M$  are 1, and the relationship reduces to

$$T = J \cdot \begin{bmatrix} \sec \varphi & 0 \\ 0 & 1 \end{bmatrix} \quad (2.9)$$

after inverting the right-side matrix. In this context, the Jacobian matrix is given as

$$J = \begin{bmatrix} \frac{\partial x}{\partial \lambda} & \frac{\partial x}{\partial \varphi} \\ \frac{\partial y}{\partial \lambda} & \frac{\partial y}{\partial \varphi} \end{bmatrix}. \quad (2.10)$$

The significance of this description is that  $T$  describes the affine transformation applied to the infinitesimal circle from the sphere that results in the Tissot ellipse on the plane. I will make use of that fact after some preparatory remarks.

Let us say we have a detailed base map prepared for use in a service deployed on the World Wide Web. We wish to accept arbitrary data sets to represent and overlay onto the base map in order to augment the map with information customized for a user's needs. The bulk of the rendering work and detail needed for the complete map has already gone into the base map, and we do not wish to render the base map anew for every custom map because we want to conserve computational resources and to reduce delivery time.

The scenario turns out to be common: Practically every large-scale mapping service on the Web serves up "tiles" rendered in advance and upon which user-specified data gets overlaid and displayed. The tiles may be raster, as in Google Maps (Rasmussen, Rasmussen, & Ma, 2011), or vector, as in Mapbox (2017), but either way, they have been prepared in advance on a specific map projection. That specific projection for the major commercial services is the "Web Mercator," which is the spherical Mercator projection. At small scales, its mathematical usage is unremarkable, but its portrayal of the world is controversial. At large scales, its portrayal of local areas is unremarkable, but its mathematical usage is controversial. As described by Battersby, Finn, Uesry, and Yamamoto (2014), small-scale controversy stems from the usual criticisms of Mercator: It shows gross area disproportion across the map. Large scale controversy stems from using geodetic coordinates as surveyed against an ellipsoidal model, but projected using the spherical Mercator. Technically, this practice makes the map slightly non-conformal, and also contrary to practice in any other context such that the US National Geospatial-Intelligence Agency felt compelled to issue an injunction against its use for Department of Defense work (US NGA 2014).

On the other hand, Web Mercator brings considerable benefits to the online mapping scenario: At local scales, any place in the world away from the poles gets treated without perceptible distortion, and therefore "fairly." North is always up, so orientation is consistent and familiar. Tiles can be rendered and stored in advance, saving time and enormous computational resources when serving up tiles. Because Mercator is locally correct everywhere, adjusting the scale bar is the only change needed for rendering when panning north-south, and no change at all is needed east-west.

By contrast, using any other projection would eliminate at least one of those benefits. In particular, if the mapping system wished to serve up an equal-area projection instead, most of the world would be horribly distorted even at local scales. In order to correct that, the mapping system would have to customize the projection's standard parallels, *at the very least*, in order to



serve up tiles fair to everyone – at huge expense for rendering if panning north–south. But most map-makers would not be pleased with simple, rectangular equal-area projections; they would want a pseudocylindric or something more elaborate, and in that case, the central meridian would also need to be adjusted and the map rendered accordingly. This means panning in any direction requires continuous re-rendering throughout the operation.

Now, consider any non-conformal projection. Because the projection is not conformal, it distorts angles across most of the map, which is why it normally cannot be used efficiently for Web map services that provide usual pan-and-zoom functionality. However, if we consider the local distortion  $T$  from Equation (2.8) as an affine transformation, we can *undo* that distortion for any particular point of interest  $p$  simply by applying  $T^{-1}(p)$  to the entire map. This would distort the rest of the map, of course, but there are two reasons why this is still reasonable: (1) When zoomed in, we do not even display those portions of the map that would be heavily distorted; and (2) Why were the undistorted parts of the original map special anyway? We have changed how distortion is distributed, but have not necessarily worsened the overall distortion. Figure 1 shows this treatment for the Wagner VII projection.

But, why would we do this? It turns out that affine transformations are *exceedingly* efficient on modern computing hardware due to the ubiquity of graphics processing units (GPUs) in desktop and mobile computers. As per Sørensen (2012) and endless other sources, affine transformations, being matrix–vector multiplications, are essentially what GPUs are made for. By offloading affine transformation from the central processing unit to the GPU, speed can be increased by several orders of magnitude. Therefore, even though a Web mapping service might construct static tiles on a particular projection in a particular aspect, it need not be bound to the original distortion characteristics. Instead, it could vary the locus of low distortion according to the progression of pan and zoom by applying, to the entire displayed portion of the map, the affine transformation that would undo distortion at the point of most interest.

Affine transformation used this way would introduce problems of its own. Marks whose shapes are not intended to be projected, such as labels or dots for cities, could not be reasonably rendered on the base maps because of the abuse they would suffer when distorted by the affine transformation. Instead, they would have to be rendered and applied after the transformation. Furthermore, in order to avoid serious

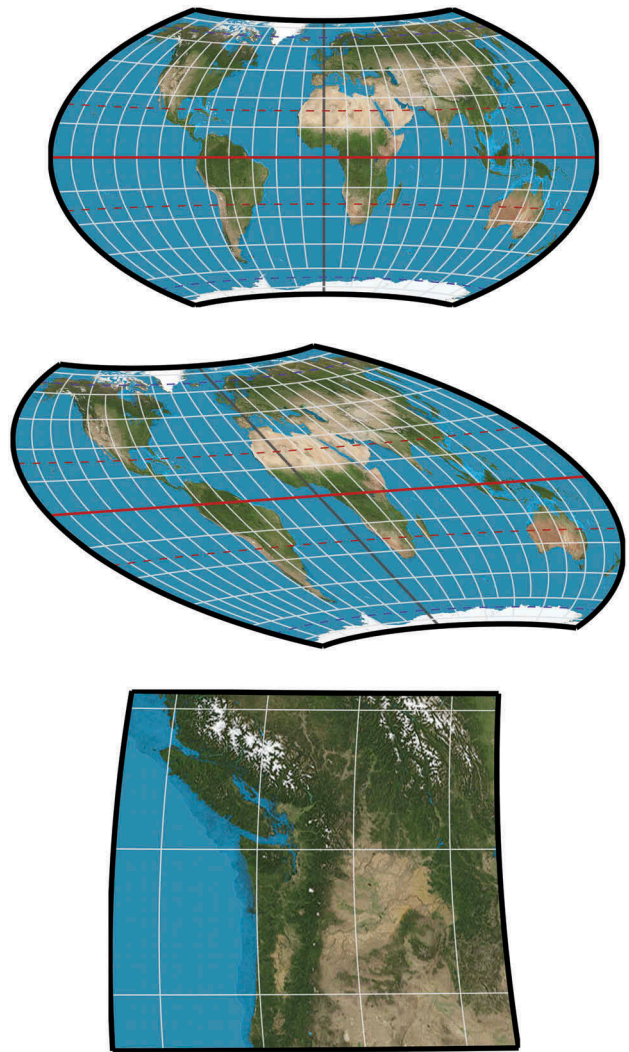


Figure 1. Wagner VII, 15° and 4° graticules, affine transformation to benefit North American Pacific Northwest (one-column).

aliasing when transforming, the original rendering would need to happen at several times the target resolution, and then be scaled down (decimated) after transforming, implying more calculation. Aside from increased computational costs, subtleties, such as label placement then get pushed to run-time, where they cannot be corrected by human intervention. Still, freeing the Web mapping service from the confines of Mercator while retaining most of the benefits of using it suggests value in this novel technique.

The need for emancipation is particularly urgent for visualizations of statistical information at small scales, where Mercator shows up frequently but wholly inaptly. According to Gartner Inc. (2017), the business intelligence and analytics market is led by Tableau, Microsoft’s Power BI, and Qlik with their visualization-based approaches to displaying business data. Displaying data on maps is important to all three

platforms, as per Gartner’s description of capabilities they deem critical for their rankings. Meanwhile, as of this writing, Tableau’s only “natively” supported projection is the Web Mercator (Dominguez, 2016); Power BI’s is also Web Mercator; and Qlik’s was until 2014, when plate carrée (“Unit” projection, in Qlik parlance) was added (Muñoz, 2015). Unfortunately, plate carrée is not much better than Mercator over most of the world that is relevant to business. All of these systems have ways to show maps in other projections, but doing so requires abandoning the system’s background map tiles. (In Power BI’s case, I found no reliable source describing the native base map projection, and so relied on my own investigations.)

### 2.3. The Bonne transform

The Bonne projection appeared in rudimentary form in the early 1500s, and was likely defined precisely by the late 1600s. It is an equal-area projection consisting of arcs of concentric circles to represent latitude, with each arc subtending the angle needed to give it proportionally correct length for the parallel it represents. One parallel  $\varphi_1$  must be chosen to have no distortion. Meridians intersect a given parallel at constant intervals. The projection is symmetric east–west. As  $\varphi_1$  approaches the equator, the Bonne approaches the sinusoidal projection. As  $\varphi_1$  approaches  $90^\circ$ , the Bonne approaches the Werner projection.

Another way to think about the projection is as an area-preserving transformation of the sinusoidal projection. To review, the sinusoidal is a pseudocylindrical projection, and, therefore, in equatorial aspect its parallels are straight lines. Each parallel has correct scale in the direction of the parallel for its entire length. To transform the projection into the Bonne, each parallel is bent into the arc of a circle without stretching it, such that each arc’s circle is concentric to the others and therefore all have a common center. The radius of the circle for any parallel’s arc ultimately is determined by the latitude chosen for  $\varphi_1$ . If  $\varphi_1$  is a low latitude, the common center will be far from the map, parallels will curve gently, and the arc subtended by each parallel will be a small fraction of its circle. If  $\varphi_1$  is the equator, the common center will be off at infinity and the arcs will be straight segments. If  $\varphi_1$  is at a high latitude, the common center will be close to the map, parallels will curve rapidly, and the arc subtended by each parallel will be a large fraction of its circle.

Thought about this way, the Bonne projection is a planar transform. What makes it unusual is that its range need not be confined to the projection itself

because we only need use longer arcs in order to extend the range, up until the point where the arc wraps back upon itself. With this extended range, the transform can be applied to arbitrary other projections even without scaling first. Therefore, the Bonne *transform* is a parameterized, equivalent planar transform, while the Bonne *projection* is an instance of that transform applied to the sinusoidal projection.

I used the Bonne transform to create a series of equal-area projections based on manipulations of existing projections. The projections are bilaterally symmetric, equal-area, and have curved parallels in equatorial aspect. Each can be parameterized by a “latitude of curvature,” which is the  $\varphi_1$  of the Bonne transform but without the meaning of a standard parallel in the resulting projection. First, I apply an affine transformation to the original projection to give it correct scale at the center. Then I interrupt the base projection along the equator by applying the Bonne transform independently to both northern and southern hemispheres, greatly reducing distortion in each hemisphere (Figure 2). As an interruption scheme, this is similar to some cordiform projections from the 16th century, such as those of Oronce Fine, 1531, “Nova, Et Integra Universi Orbis Descriptio,” or Gerard Mercator, 1538, untitled double cordiform map as copied by Antonio Salamanca, c. 1550. However, whether the motivation was the same or not is unclear. Those earlier forms were not equal-area and arose out of geometric construction rather than planar transformation.

As found in Geocart 1.2 (1992), a commercial map projection software package I authored, originally I did not split the equator all the way to the central meridian. Instead, after centering the map at  $11^\circ\text{E}$  to prevent separating the Chukchi peninsula, I interrupted along the equator from the left edge eastward  $90^\circ$  through the Pacific, and split the same distance inward from the east edge. The central portion of the map remained unchanged, while the eastern and western outer wings of the northern hemisphere curled upward from the cusps of the interruptions, and likewise downward for the southern. By means of the partial interruption, the map avoided slicing major land masses.

I achieved the partial interruption by applying the left half of the Bonne transform to the leftmost  $90/360$  of the map, and the right half of the Bonne transform to the rightmost  $90/360$  of the map. A vertical line struck at the inner limit of each equatorial interruption became the “central meridian” for each of the half-Bonne transforms.

This procedure yielded a smooth, equal-area map. However, as a piecewise function, the projection could not have continuous derivatives and therefore its

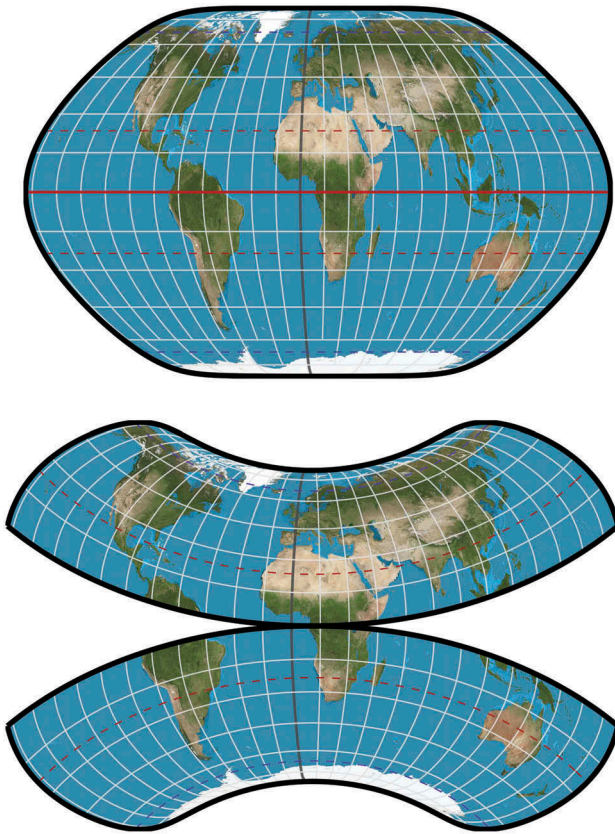


**Figure 2.** 15° graticules and centered at 11°E.

Top: Minimum-error pointed-pole equal-area projection (Snyder, 1985, p. 128). Bottom: Affine scaling to correct center scale, and Bonne transform applied with  $\varphi_1 = 22^\circ$  (one-column).

distortion characteristics must change abruptly. I abandoned partial interruption for this projection series starting with Geocart 2.0 (1994). Nevertheless, this application of the Bonne transform to only parts of a map emphasizes its nature as a “transform,” more than a “projection,” and also illustrates that planar transforms can be applied piecewise to portions of the full equal-area map if convenient. This flexibility is unavailable to conformal maps because a transformation of a conformal map that yields a continuous mapping necessarily affects the entire map.

#### 2.4. Directional path offset

Affine transformation in the most general sense can be thought of as a combination of scaling independently in both directions, rotating around the origin, and shearing. Shearing is the operation that turns a rectangle into a rhombus. As an affine operation, shearing too, preserves area. A conceptual model for shearing’s area preservation will be helpful. Considering a rectangle we wish to shear such that it leans rightward, we can break the rectangle up into an infinite number of

slivers as rectangles of the same width and infinitesimal height. We leave in place the sliver at the base of the original rectangle. We slide all the slivers above it an infinitesimal distance to the right. Then we hold the sliver next to the base sliver fixed, and slide everything above it again by the same amount. Then we hold the next sliver up fixed, and repeat, all the way up to the top sliver. It should be clear that area has not changed, since we kept each sliver the same length and (infinitesimal) height, and opened no extra space between them.

Notice that the concept for area preservation holds regardless of whether the shift amount is constant or otherwise. In other words, we can deform that rectangle into other shapes besides rhombi while preserving area. We must be careful not to open up space between the slivers, or skew them with respect to each other; we may only slide them against each other, all in parallel. If we honor those conditions, we can define an arbitrary path for that left edge. The same argument holds for pressuring the original rectangle from *any* constant direction, not just against one of its edges. Applying this principle to the projection of Figure 2, we arrive at Figure 3.

I used this technique in a National Geographic animation (Strebe, Gamache, Vessels, & Tóth, 2012), in order to progressively close up the interruptions in the closing sequence featuring a Mollweide projection. The projection remains equal-area throughout. I also exploited this technique in the 1992 series mentioned in Section 2.3. In their original form wherein the equatorial interruption was only partial, the option to close up the interruptions or leave the map interrupted was available. When I abandoned partial interruption in favor of the full interruption, I eliminated the option to show the projections as interrupted from Geocart, which now always uses the directional path offset to close them up. The projections still appear in the extant Geocart 3.2 (2018) in the closed-up form, but were never formally described. They are shown here as Figure 4. The meridians of those projections are kinked at the equator as a consequence of the manipulation, a typical, undesirable side effect of directional path offsets when used to close interruptions.

#### 2.5. Meridian duplication

Aitoff (1892) introduced a brilliant little device that may have been the first prominent sphere-to-sphere transformation for cartographic maps. His invention was to halve the longitudinal value of every location on the sphere, squeezing the sphere into one



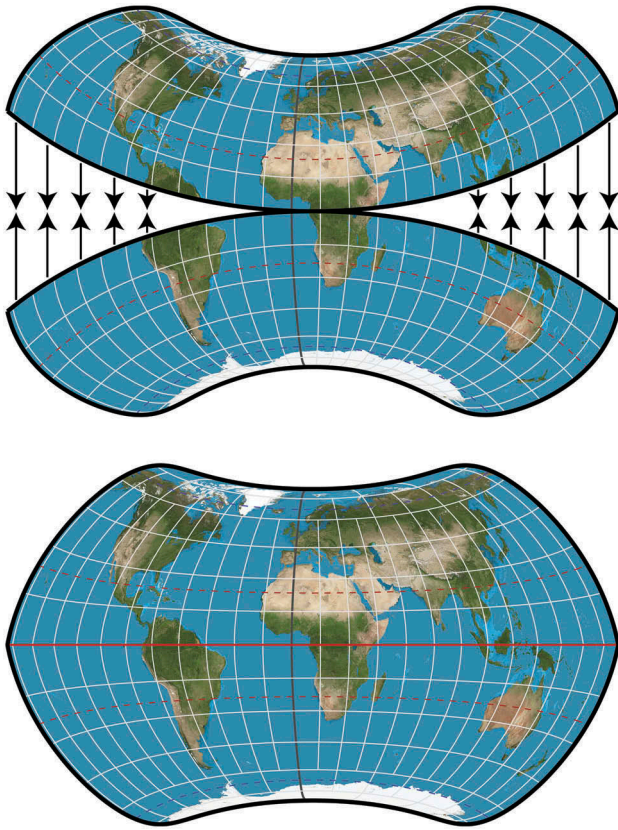


**Figure 3.** 15° graticules and centered at 11°E. Application of directional path offset to close interruption (one-column).

hemisphere. Then, after projecting the hemisphere onto the plane as an equatorial azimuthal equidistant, the method stretches the map horizontally 2:1 in order to compensate for the squeezing on the sphere. By these means he created the Aitoff projection, a simple,

elliptical, pseudoazimuthal projection that reduces shearing compared to the similar pseudocylindric Apian II projection by gently curving the parallels. Aitoff published the first map on the projection in *Atlas de géographie moderne* in 1889.

Aitoff's invention soon inspired Hammer (1892) to pull the same trick on the Lambert azimuthal equal-area projection. Hammer's insight was that Aitoff's sphere-to-sphere transform preserves areas because the squeezing on the sphere maintains a constant relationship between the differential properties defining the area metric on the sphere. Therefore, projecting the squeezed sphere onto the plane via an equal-area projection must result in an equal-area projection. Scaling, as noted in Section 2.1, also preserves area, and so the resulting projection must be equivalent. The Hammer projection has seen much use as a curved-parallel alternative to the pseudocylindric Mollweide in much the same way that the Aitoff is a curved-parallel alternative to the Apian II. Startlingly, despite the Hammer projection's favorable properties, it is computationally much cheaper than the Mollweide because it requires no iteration.

Hammer chose  $n = 1/2$  to multiply longitudes by in his formulation, but over the years a few other values for  $n$  were proposed, such as Rosén's  $7/8$  or Eckert-Greifendorff's  $1/4$ . Briesemeister proposed an oblique case of the Hammer with change in aspect ratio (Snyder, 1993, pp. 236–240).

The Bonne projection, especially its specialization in the form of Werner ( $\varphi_1 = 90^\circ$ ), frequently appears as a novelty to show the world in a heart, with equivalence as a bonus. Dissatisfied with the shape's aesthetics, I

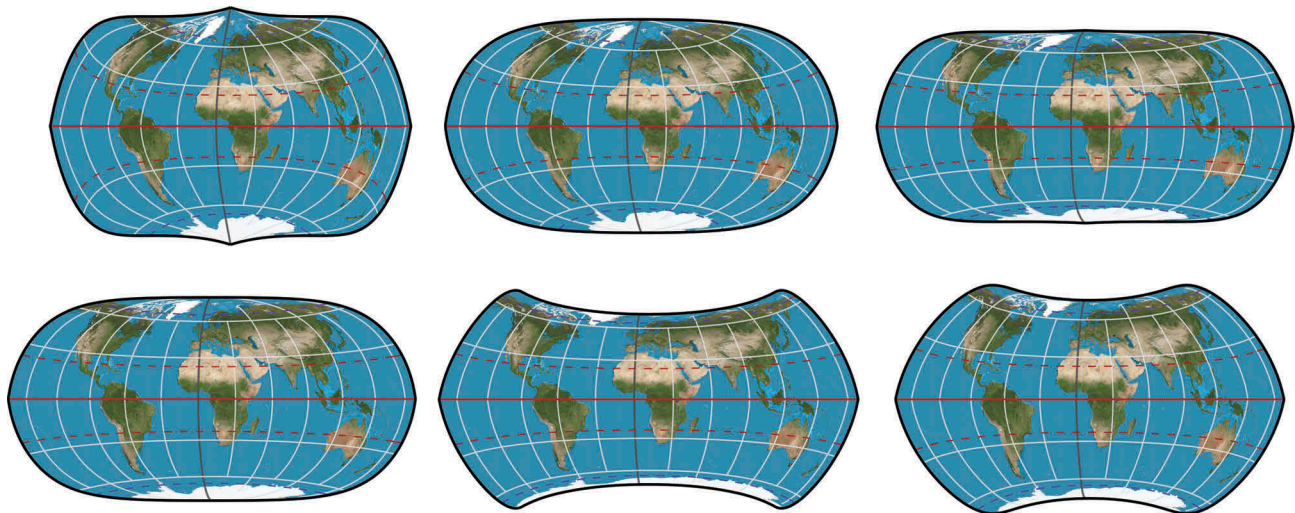


**Figure 4.** 30° graticules and centered at 11°E; Bonne  $\varphi_1$  in parentheses.

Top: Strebe-sinusoidal ("cartouche") (25°44'16"), Strebe-Hammer (15°), Strebe-Kavraiskiy V (16°27'). Bottom: Strebe-Mollweide (16°), Strebe-Snyder flat-pole (20°), Strebe-Snyder pointed-pole (22°) (two-columns).



devised a variant by 1992 and incorporated it into Geocart 1.2 as simply the “heart” projection. It has not been otherwise described. I observed that “meridian duplication,” as I call Aitoff’s innovation, would suffice to modify the Bonne into a more or less idealized heart shape. The projection permits configuration via  $\varphi_1$  of the Bonne and the meridian duplication factor, set by default to  $85^\circ$  and  $6/5$ , respectively (Figure 5). My convention for the meridian duplication factor is the reciprocal of  $n$  given above in Hammer’s formulation and below in Wagner’s, and happens to coincide with that of Snyder (1993, p. 236).

Kronenfeld (2010) also uses meridian duplication in developing a simple sphere-to-sphere transformation. In Kronenfeld’s case, longitudes are expanded with the intent of projecting a fraction of the globe onto a larger section of the globe while preserving areas. Kronenfeld refers to this as “longitudinal expansion factor.” This procedure must discard regions of the globe; otherwise parts would wrap and overlap. With  $n$  as above,  $\alpha$  as the desired magnification,  $\lambda_0$  as the “reference meridian,” and  $\varphi_1$  as the “reference parallel” (together constituting the “origin,” in a sense), the transformed spherical coordinates  $(\varphi', \lambda')$  are given as

$$\begin{aligned}\sin \varphi' &= \frac{\alpha}{n} (\sin \varphi - \sin \varphi_1) + \sin \varphi_1, \\ \lambda' &= \lambda_0 + n(\lambda_0 - \lambda).\end{aligned}\quad (2.11)$$

How (or whether) the transformed spherical coordinates then get projected to the plane is up to the projection designer. I note that Kronenfeld’s transform is the equivalent of excerpting a rectangle from a cylindrical equal-area projection, scaling it, translating it on the plane to center it at projected  $(\varphi_1, \lambda_0)$ , and deprojecting

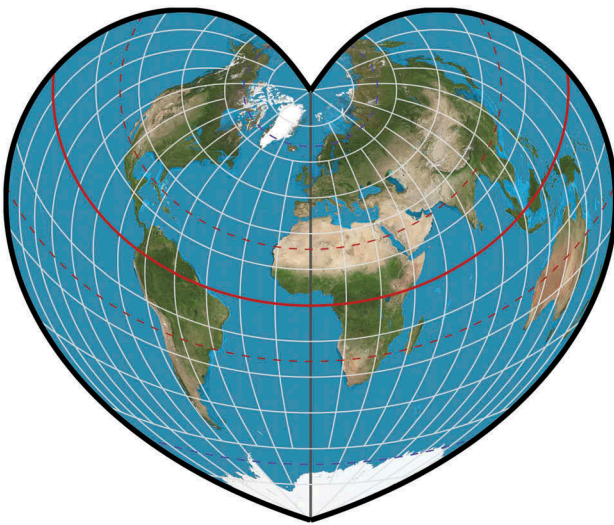


**Figure 5.** Strebe’s heart projection,  $\varphi_1 = 85^\circ$ , “meridian duplication factor” =  $6/5$ , or  $n = 5/6$  (one-column).

back to the sphere via the inverse of another cylindrical equal-area projection. Each of these steps is noted individually in this paper.

## 2.6. Das Umbeziffern

Wagner (1932) generalized Aitoff’s notion to reassign not only longitudinal values, but latitudinal values as well. He called the procedure *Umbeziffern*, or “renumbering,” referring to the reassignment or relabeling of the longitude and latitude values. The theory was developed in depth by Karl Siemon over a series of papers in 1936–8 and then deployed by Wagner over the course of his life in the development of many texts and projections, starting in 1941 (Canters, 2002, pp. 119–124). Wagner and Siemon’s explications went beyond just equal-area projections to accommodate several constraints, but what concerns us here is the equivalence transformation, which Canters refers to as Wagner’s second transformation method. Presuming that

- $0^\circ\text{N}, 0^\circ\text{E}$  projects to  $x = 0, y = 0$ ;
- $f_1$  denotes the base projection’s generating function for  $x$ ;
- $f_2$  denotes the base projection’s generating function for  $y$ ;
- $x', y'$  are the coordinates produced by Wagner’s second transformation;
- $n$  is the fraction to multiply longitudes by;
- $k$  is a desired scaling (such as to eliminate distortion at selected parallel at central meridian);
- $m$  is a free parameter

then,

$$x' = \frac{k}{\sqrt{mn}} f_1(u, v), \quad y' = \frac{1}{k\sqrt{mn}} f_2(u, v), \quad (2.12)$$

where  $v = n\lambda$ ,  $\sin u = m \sin \varphi$ .

Besides those of Wagner himself, projections using Wagner’s method were devised by Böhm (2006). Šavrič and Jenny (2014) present an adaptable pseudocylindrical projection from Wagner’s method, and Jenny and Šavrič (2017) use it to transition between Lambert azimuthal equal-area and a transverse cylindrical equal-area in order to improve the adaptive projection system Jenny (2012) describes.

## 2.7. Slice-and-dice

The differential forms that identify a projection as equivalent are not conducive to generating new projections. Given suitable constraints and boundary conditions, it can be done, but in the general case requires

nested integrals with the implication of enormous computational cost. Most of the techniques described in this work are, in essence, ways to avoid dealing directly with the infinitesimals.

Van Leeuwen and Strebe (2006) describe a mechanism for approaching the two-dimensional problem of area preservation one dimension at a time. While we only applied the method in the context of polyhedral faces, it is generally applicable. Our work proves that you can reach the differential qualifications of an equal-area projection by slicing up the space in one direction (or dimension) such that each slice has the correct area, and then dicing up the slices in a different direction (or dimension) such that the second dimension's dices also preserve areas. The two directions need not be orthogonal – and cannot be everywhere – but the results will still retain equivalence. The paper generalizes an earlier projection by Snyder (1992) and provides a theory for it.

Any equal-area projection can be thought of in these terms. For example, finding the position of a latitude in the well-known Mollweide projection can be thought of as slicing the ellipse with a straight, horizontal parallel placed so that the proportion of the global area higher in latitude is correct with respect to the global area lower in latitude, and then dicing up the same space with meridians whose spacing is constant along the parallel. The dice condition of constant spacing is forced by how we chose to slice.

More as a way of thinking about equal-area projections than a “technique,” slice-and-dice has no general formulae to resort to, and in many cases provides no shortcut to a solution. Van Leeuwen and I used it in the context of our work because the great- and small-circle partitions we explored sliced and diced the space in computationally efficient ways. I do not explore the technique further here but instead refer the reader to the 2006 paper for proof of the concept and applications.

## 2.8. Substitute deprojection

As noted in Šavrič, Jenny, White, and Strebe (2015) in describing the “Strebe transformation,” an equivalent mapping from the sphere back onto the sphere can be created by projecting from sphere to plane while preserving areas and then deprojecting back onto the sphere by means of some other equal-area projection's inverse. This is a sphere-to-sphere mapping mediated by projection onto the plane. The result may then be projected again to the plane by means of yet another equal-area projection. A reason to do this is to draw upon the vast corpus of extant equal-area projections.

After the Bonne transform experiments that resulted in the projections of Figure 4, I considered ways to eliminate the unsatisfactory discontinuity at the equator without changing the other characteristics. Noting that Mollweide and Hammer share the same projection space and are both equal-area, I conceived of a vector space that transforms Mollweide to Hammer, with the intent of applying that vector space to other equal-area projections. This readily generalizes to the observation that any portion of an equal-area projection  $A$  could be treated as if it were a portion of any other equal-area projection  $B$ , thence deprojected back onto the sphere via  $B$ 's inverse  $B'$ , and finally projected back to the plane by yet another projection  $C$  in order to arrive at a final projection  $D$ . Affine transform  $X$  is permissible between  $A$  and  $B'$  if needed for  $A$ 's domain to fit within  $B$ 's confines or even just to change how much of  $B$  impacts  $A$ . Affine transformation at that stage normally would be counteracted by its inverse after projecting via  $C$ , and so the full sequence would look like this:

$$D = X^{-1}C(B'[X \cdot A]). \quad (2.13)$$

Ultimately, I chose Eckert IV as  $A$ , Mollweide as  $B$ , and Hammer as  $C$ . For  $X$  I chose

$$X = \begin{bmatrix} \frac{1}{2}s & 0 \\ 0 & \frac{1}{s} \end{bmatrix} \quad (2.14)$$

with  $s = 1.35$  recommended.

Collected, this is the formulation of the Strebe 1995 projection (Figure 6):

$$x = \frac{2D}{s} \cos \varphi_p \sin \lambda_p, \quad y = sD \sin \varphi_p$$

$$s = 1.35$$

$$D = \sqrt{\frac{2}{1 + \cos \varphi_p \cos \lambda_p}}$$

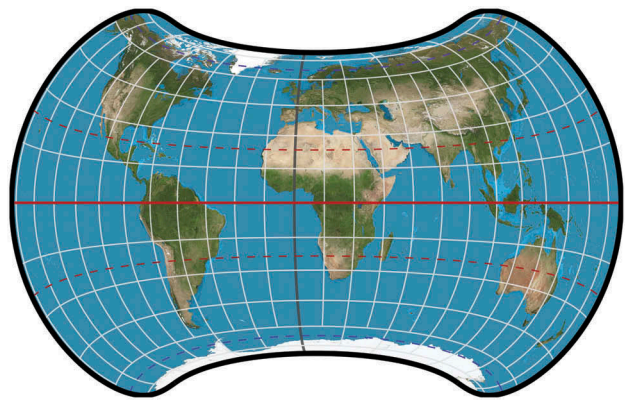


Figure 6. Strebe 1995 projection, 15° graticule and centered at 11°E,  $s = 1.35$  (one-column).

$$\begin{aligned}\sin \varphi_p &= \frac{2 \arcsin \frac{\sqrt{2}y_e}{2} + ry_e}{\pi} \\ \lambda_p &= \frac{\pi x_e}{4r} \\ r &= \sqrt{2 - y_e^2} \\ x_e &= s \frac{\lambda(1 + \cos \theta)}{\sqrt{4\pi + \pi^2}}, \quad y_e = 2 \frac{\sqrt{\pi} \sin \theta}{s\sqrt{4 + \pi}},\end{aligned}$$

where  $\theta$  is solved iteratively:

$$\theta + \sin \theta \cos \theta + 2 \sin \theta = \frac{1}{2}(4 + \pi) \sin \varphi.$$

As quoted by Raposo (2013), my goals for the projection design were to preserve area; maintain bilateral symmetry; and push as much distortion as feasible into the oceans and away from the land masses without resorting to interruptions. Geographer Marina Islas, who used the projection for a map tattooed on her upper back, appreciated it for its organic shape and Afro-centric presentation (Zimmer, 2011, pp. 90–91; New York Times, 2011, image in online review).

Šavrič et al. (2015) used substitute deprojection in constructing novel map projections for a study of map reader preferences with regard to map projection aesthetics. One of their hypotheses was that map readers would prefer projections whose outer corners  $\theta$  are softer, or rounder. To test the hypothesis, they developed a Wagner VII with rounded corners and a Miller with rounded corners. (Though the substitute deprojection they used does preserve areas, that particular benefit was lost on the Miller projection, which is not equivalent.)

## 2.9. Strebe's homotopy

Strebe (2017) describes an efficient method for synthesizing a continuum of equal-area projections between any two chosen equal-area projections. A parameterized continuum between two projections is known as a *homotopy* in algebraic topology and related fields. The need for such a continuum arose in the context of Jenny's efforts to improve his adaptive composite projection system of 2012, where no good transition from Lambert azimuthal equal-area to a transverse cylindrical equal-area projection had been found. While the system I devised then solved the immediate need, its applicability is far more general: It can produce a continuum between two arbitrary projections with few restrictions, whether equal-area, conformal, mixed, compromise, or otherwise. If both the initial and terminal projections are equal-area, the result will be equal-area. If both are conformal, the result will be conformal. The general description is the same regardless:

$$C = B(A'[k \cdot A])/k, \quad (2.15)$$

where  $C$  is the “weighted average” projection;  $A$  is the initial projection;  $A'$  is its inverse;  $B$  is the terminal projection; and  $0 \leq k \leq 1$  is the weighting. (As  $k \rightarrow 0$ , this formulation should be taken as a limit.) This process includes a substitute deprojection in the form of  $A'(k \cdot A)$ .

In the context of equal-area projections, Equation (2.15) may not suffice because the point on the plane  $P = k \cdot A$  as  $k \rightarrow 0$  might not be undistorted for the given  $A$ . If  $A(P)$  is distorted, then Formula 2.15 will not result in  $A$  as  $k \rightarrow 0$  because  $A'(P)$  back onto the sphere would undo the original distortion. A simple, failsafe way to attain  $A$  in that situation is to apply an affine transformation  $M_A$  to the result to reassert the original distortion. The strength of  $M_A$  must wane as  $k$  progresses away from 0. One formulation of  $M_A$ , not unique, is

$$N_a = k \cdot I + (1 - k) \cdot T_A(P)$$

$$M_A = \frac{N_A}{\sqrt{\det N_A}}, \quad (2.16)$$

where  $T_A$  means the Tissot transformation at  $A(P)$  from Equation (2.8), and  $I$  is the identity matrix.

Likewise, if  $B(P)$  is distorted, then Equation (2.15) will not suffice because  $B(A'[k \cdot A(P)])$  asserts  $B$ 's distortion even when  $k = 0$ , where we expect  $C = A$ . We could correct that by reversing the distortion of  $B(P)$  by applying an affine transformation  $M_B$ . One formulation, not unique, is

$$N_B = k \cdot I + (1 - k) \cdot T_B^{-1}(P)$$

$$M_B = \frac{N_B}{\sqrt{\det N_B}}. \quad (2.17)$$

The general expression for equal-area homotopies then becomes

$$C = M_A \cdot M_B \cdot B(A'[k \cdot A])/k. \quad (2.18)$$

Homotopies generated by this method are asymmetric; that is, reversing  $A$  and  $B$  and replacing  $k$  with  $1 - k$  in the formulation will not result in the same  $C$ . In my 2017 work, I demonstrate both directions of homotopy between Albers and Lambert azimuthal equal-area for the full sphere. The method worked well despite the very different topologies of a conic and an azimuthal projection. Figure 7 gives another example, comparing my homotopy method to my adaptable equal-area pseudoconic projection (itself a homotopy) that hybridizes Albers and Bonne (Strebe, 2016). Despite the markedly different methodologies, practically identical results can be obtained because of



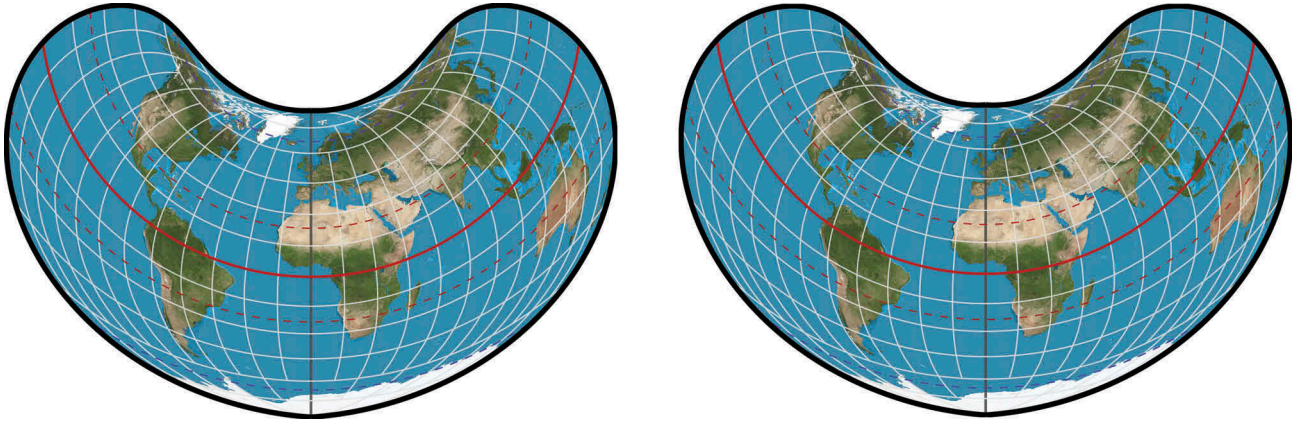


**Figure 7.** 15° graticules on Bonne-Albers homotopies. Left: Strebe homotopy,  $k = 1/2$ ,  $\varphi_1 = 29^\circ 30'$ ,  $\varphi_2 = 45^\circ 30'$ ,  $\varphi_3 = 37^\circ 4' 24''$ ; Right: adaptable equal-area pseudoconic,  $k = 0.47$ ,  $\varphi_1 = 10^\circ$ ,  $\varphi_2 = \varphi_3 = 40^\circ$  (two-columns).

the number of degrees of freedom available in parameterization.

Strebe's homotopy uses substitute deprojection at the level of infinitesimals. In that sense it is both a generalization of, and a specialization of, substitute deprojection. Generalization, because it extends the concept into an area-preserving calculus; specialization, in that only two of the three projections are independent of each other, as well as because it imposes a sharply defined goal onto the procedure: homotopy. Substitute deprojection on its own, meanwhile, imposes no goal other than the synthesis of new equal-area projections out of existing ones.

### 2.10. Axial yanking

I developed this technique as a generalization of scaling. If we pick an axis for the projection (often the central meridian or the equator on an equatorial aspect with bilateral symmetry), we can choose a function  $f$  to apply to the partial derivatives of the projection in the direction of that axis. Considering a given point  $P$  along the axis, insofar as we apply the reciprocal of that evaluated function  $f$  to every point perpendicular to the axis from  $P$ , we will have arrived at a new equal-area projection. In a sense, we scale each parallel line (geometrically parallel, not parallels of latitude) by a different amount.

Let me illustrate with the Hammer projection. Reviewing its generating functions (after Snyder, 1989, p. 232):

$$D = \sqrt{2}(1 + \cos \varphi \cos n\lambda)^{-\frac{1}{2}}$$

$$x = \frac{D}{n} \cos \varphi \sin n\lambda, \quad y = D \sin \varphi, \quad (2.19)$$

where  $n = \frac{1}{2}$  is the meridian duplication factor Hammer chose. Partial derivatives relevant later are:

$$\frac{\partial x}{\partial \lambda} = \frac{\sqrt{2}}{2} z \cos \varphi (\cos \varphi \cos^2 n\lambda + \cos \varphi + 2 \cos n\lambda) \quad (2.20)$$

$$\frac{\partial y}{\partial \varphi} = \frac{\sqrt{2}}{2} z (\cos^2 \varphi \cos n\lambda + 2 \cos \varphi + \cos n\lambda) \quad (2.21)$$

$$z = (1 + \cos \varphi \cos n\lambda)^{-\frac{3}{2}}.$$

The Hammer projection has no distortion at the center, but is distorted everywhere else, including along the central meridian and along the equator. Let us suppose we want a similar projection but with an undistorted central meridian. To achieve this, we can “yank” the vertical axis to be undistorted by letting  $f$  discussed above be the reciprocal of Equation (2.21). However, we do not need to evaluate that explicitly because we chose  $f$  such that  $y$  would be  $\varphi$  along the central meridian. That is,  $\partial y / \partial \varphi$  will be 1 along the central meridian.

Here is how to express that. Given  $H$  as the Hammer projection definition, for every  $[x_c, y_c] = H(\varphi_c, \lambda_c)$  projected coordinate, find  $\varphi_{CM}$  such that  $[0, y_c] = H(\varphi_{CM}, 0)$ , and then force  $y = \varphi_{CM}$ . Next, in order to preserve equivalence, multiply  $x_c$  by  $\frac{\partial}{\partial \varphi} H(\varphi_{CM}, 0)$  because we implicitly divided the infinitesimal height of the entire line  $y_c$  by that value when we set  $y = \varphi_{CM}$ .

Finding  $y_c = H(\varphi_{CM}, 0)$  means needing the inverse for the  $y$  value of  $H$ , but only along the central meridian such that  $\lambda = 0$ :

$$y_c = \sqrt{2} \sin \varphi_{CM} (1 + \cos \varphi_{CM})^{-\frac{1}{2}}. \quad (2.22)$$

Solving for  $\varphi_{CM}$ ,

$$\varphi_{CM} = \operatorname{sgn}(y_c) \arccos \left( 1 - \frac{1}{2} y_c^2 \right). \quad (2.23)$$

At  $\lambda = 0$ , simplifying Equation (2.21),

$$\frac{\partial}{\partial \varphi} H(\varphi, 0) = \frac{\sqrt{2}}{2} \sqrt{\cos \varphi + 1} \quad (2.24)$$

which, when  $\varphi = \varphi_{\text{CM}}$  as per Equation (2.23), is

$$\frac{\partial}{\partial \varphi} H(\varphi_{\text{CM}}, 0) = \frac{1}{2} \sqrt{4 - y_c^2}. \quad (2.25)$$

Consolidated, Hammer with vertical axis yanked to eliminate the axis distortion is,

$$\begin{aligned} x &= x_c \cdot \frac{1}{2} \sqrt{4 - y_c^2}, \\ y &= \text{sgn}(y_c) \arccos\left(1 - \frac{1}{2} y_c^2\right) \end{aligned} \quad (2.26)$$

with  $[x_c, y_c]$  as  $[x, y]$  from 2.19.

Using the same concepts, we could, instead, yank the horizontal axis to have no distortion. This makes use of Equation (2.20) instead of 2.21, but follows a substantially similar derivation. Abbreviating,

$$\begin{aligned} x &= \frac{\text{sgn}(x_c)}{n} \arccos\left(1 - \frac{1}{2} n^2 x_c^2\right), \\ y &= y_c \cdot \frac{1}{2} \sqrt{4 - n^2 x_c^2}. \end{aligned} \quad (2.27)$$

But, why stop there? Because the vertical operation does not affect the horizontal axis, and vice versa, we can apply both in succession to render both the vertical and horizontal axes without distortion. Not surprisingly, this last projection is much like the sinusoidal but with curved parallels. Which gets applied first does matter, but the difference is small across the full allowable range of  $n$ . Whether one axis or both get straightened, I call this family of projections “hamusoidal.” It appears as [Figure 8](#).

Noting that we can parameterize Hammer with a choice of  $n$  and still yank the horizontal axis to constant scale, we can pair a northern hemisphere having one parameterization with a southern hemisphere

having a different parameterization while retaining continuity across the equator. Doing so, I arrived at the whimsical equal-area “kiss” projection of [Figure 9](#).

We eliminated distortion along an axis in these examples, yielding a side effect of computational simplicity. However, as noted at the top of this subsection, what we are really doing is applying some function to the partial derivatives along the axis. The resulting axis is the integral of those partials. If we want something other than constant scale along an axis, we would chose  $f$  to be something other than the reciprocal of the partial derivative. I do not explore that further here other than to note the obvious flexibility and easy integrability of polynomials as a distortion function.

### 2.11. Radial oozing

An azimuthal projection in north polar aspect has the basic form

$$\begin{aligned} \theta &= \lambda - \frac{\pi}{2}, \quad \rho = g(\varphi), \text{ whence} \\ x &= \rho \cos \theta, \quad y = \rho \sin \theta. \end{aligned} \quad (2.28)$$

If we generalize the system such that  $\rho$  becomes a function of both  $\varphi$  and  $\lambda$ , and such that  $\theta$  becomes a function of  $\lambda$ , we have

$$\theta = f(\lambda), \quad \rho = g(\varphi, \lambda). \quad (2.29)$$

The consequence of this relaxation is that meridians remain straight, but angles between them vary, and parallels are no longer described by circles.

We wish to constrain this system to be equal-area. As given by [Strebe \(2016\)](#), the general condition for equivalence in polar coordinates from a spherical model is

$$\rho \left( \frac{\partial \theta}{\partial \varphi} \frac{\partial \rho}{\partial \lambda} - \frac{\partial \theta}{\partial \lambda} \frac{\partial \rho}{\partial \varphi} \right) = \cos \varphi. \quad (2.30)$$

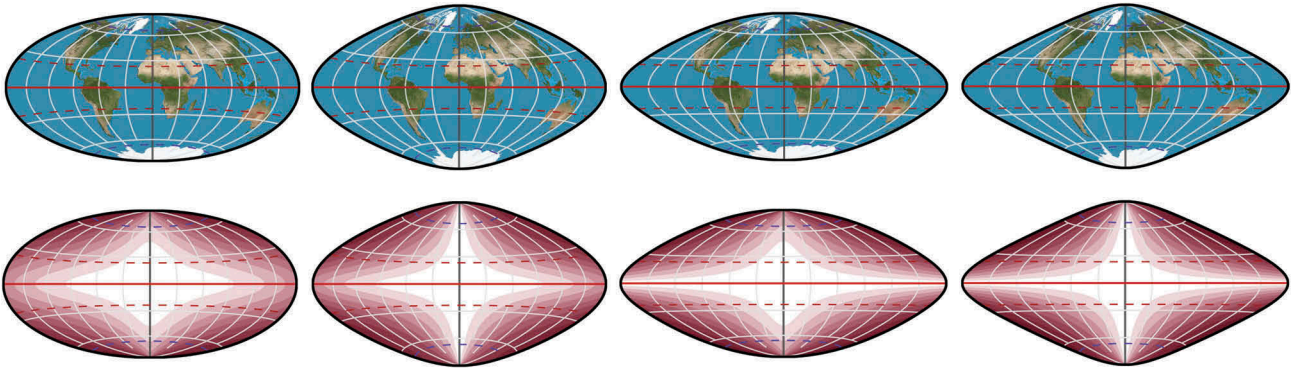


**Figure 8.** Hamusoidal,  $n = 12$ ,  $30^\circ$  graticules,  $10^\circ$  increments in angular deformation. Left to right: Hammer; vertical axis undistorted; horizontal axis undistorted; both axes undistorted (two-columns).

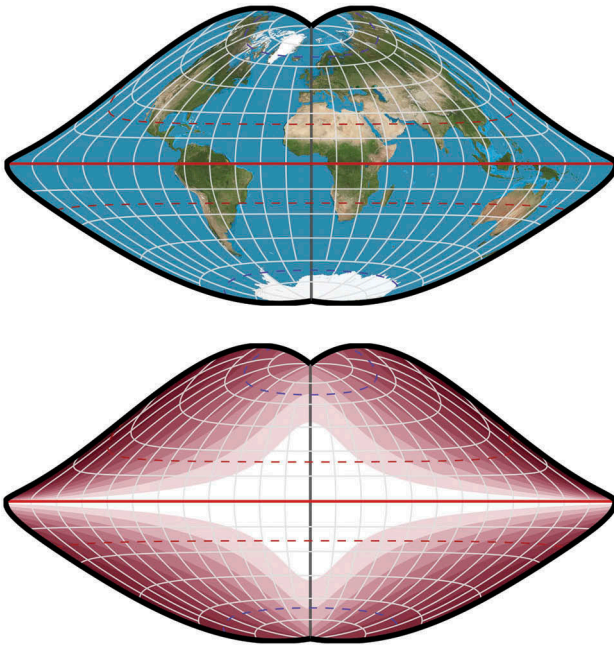


**Figure 9.** “Kiss” projection, hamusoidal north  $n = 0.85$ , south  $n = 0.65$ .  $15^\circ$  graticule,  $10^\circ$  increments in angular deformation (one-column).

In this case,  $\partial\theta\partial\varphi = 0$  because  $\theta$  is a function solely of  $\lambda$ , and therefore

$$-\rho \frac{\partial\theta}{\partial\lambda} \frac{\partial\rho}{\partial\varphi} = \cos\varphi. \quad (2.31)$$

This is not fully constrained; conic and pseudoconic equal-area projections also satisfy this differential equation because  $\partial\rho/\partial\lambda = 0$  in those cases. What we wish to do here is to squish a Lambert azimuthal equal-area projection so that it oozes into some shape other than circular. A way to do this that meets the criteria set out above is to require that all parallels retain the proportion of their spacing along the meridians, while meridians themselves vary in length. This implies that  $\rho$  is the same as Lambert’s, but shrunk or expanded by some function  $h$  that depends only on  $\lambda$  or  $\theta$ , with  $\partial\rho/\partial\varphi$  inheriting the same dependency. Lambert’s  $\rho$  is given by  $2 \sin\left(\frac{\pi}{4} - \frac{\varphi}{2}\right)$ . Substituting into Equation (2.31),

$$\begin{aligned} & -h \, 2 \sin\left(\frac{\pi}{4} - \frac{\varphi}{2}\right) \frac{\partial\theta}{\partial\lambda} \frac{\partial}{\partial\varphi} \left[ h \, 2 \sin\left(\frac{\pi}{4} - \frac{\varphi}{2}\right) \right] \\ & = \cos\varphi, \end{aligned} \quad (2.32)$$

whence

$$\frac{\partial\theta}{\partial\lambda} = h^{-2}(\lambda) \quad \text{or} \quad \frac{\partial\lambda}{\partial\theta} = h^2(\theta) \quad (2.33)$$

(depending on whichever is convenient for the projection designer’s specification for the projection), and therefore

$$\theta = \int h^{-2}(\lambda) d\lambda \quad \text{or} \quad \lambda = \int h^2(\theta) d\theta. \quad (2.34)$$

If we specify our projection via the shape we want for the outer boundary, presumably we express the shape in terms of  $\rho$  around the full sweep of  $\theta$ , or in cartesian coordinates to cast into those polar coordinates. We know how to proportion the parallels along any meridian implied by  $\rho(\theta)$ ; all that is left is to determine the meridional spread thus implied. This is available from Equation (2.34). You might have noticed that this turns  $\rho$  into a mixed-up function of  $\varphi$  and  $\theta$  from  $\varphi$  and  $\lambda$ , but because  $\theta$  has no dependence on  $\varphi$  and is invertible with  $\lambda$ , nature will ignore the transgression.

As an example, let us deform the Lambert azimuthal equal-area projection into an equal-area square. We will define the perimeter in terms of  $\rho$  and  $\theta$ , where  $\rho = h(\theta)2 \sin\left(\frac{\pi}{4} - \frac{\varphi}{2}\right)$ . The perimeter is not a continuous function because of the corners, so instead we will treat only the 0th octant  $\theta = [0, \frac{\pi}{4})$  here, with the remaining even octants being a rotation of the 0th octant and the odd octants being a reflection plus rotation of the 0th octant. The area of a sphere of unit radius is  $4\pi$ , so each side of a square of that area has length  $2\sqrt{\pi}$ . Simple trigonometry yields

$$h(\theta) = \frac{\sqrt{\pi}}{2} \sec\theta \quad (2.35)$$

and therefore, by Equation (2.34),

$$\begin{aligned} \lambda &= \int \frac{\pi}{4} \sec^2\theta d\theta \\ &= \frac{\pi}{4} \tan\theta, \text{ whereby} \end{aligned}$$

$$\theta = \arctan\left(\frac{4}{\pi}\lambda\right) \text{ and, as noted before,}$$

$$\begin{aligned} \rho &= 2h(\theta) \sin\left(\frac{\pi}{4} - \frac{\varphi}{2}\right) \\ &= \sqrt{\pi} \sec\theta \sin\left(\frac{\pi}{4} - \frac{\varphi}{2}\right) \end{aligned}$$

$$x = \rho \cos\theta, \quad y = \rho \sin\theta. \quad (2.36)$$

I show the result in Figure 10. Many years ago, in a personal communication from Waldo Tobler, I received a plotted projection that is apparently identical. However, nothing about the context remains. Tobler (2008) notes, “It is relatively easy to fit equal area maps into regular  $n$ -sided polygons,” and illustrates the pentagonal case, but does not give formulae.



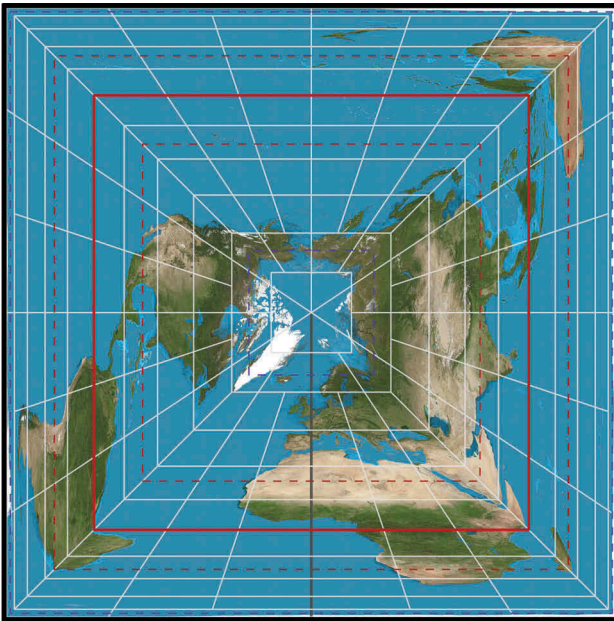


**Figure 10.** “Quasi-azimuthal equal-area square” projection,  $15^\circ$  graticule,  $10^\circ$  increments in angular deformation (one-column).

Using these same principles, I developed the whimsical “quasi-azimuthal equal-area apple,” shown in Figure 11, appearing in *Geocart 1.2* (1992). The outer boundary is described piecewise as conic sections, the piecewise nature of which accounts for the discontinuities in the distortion diagram. The boundary description is too involved to present here.

I use “quasi-azimuthal” to mean a projection which, in polar aspect, has straight meridians without constant angular separation between them. Recognizing that a region boundary on an equal-area projection says nothing about the region’s interior, it follows that an

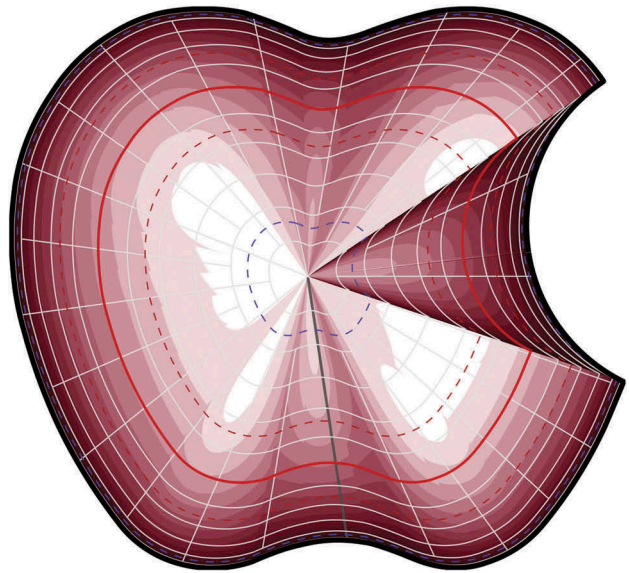
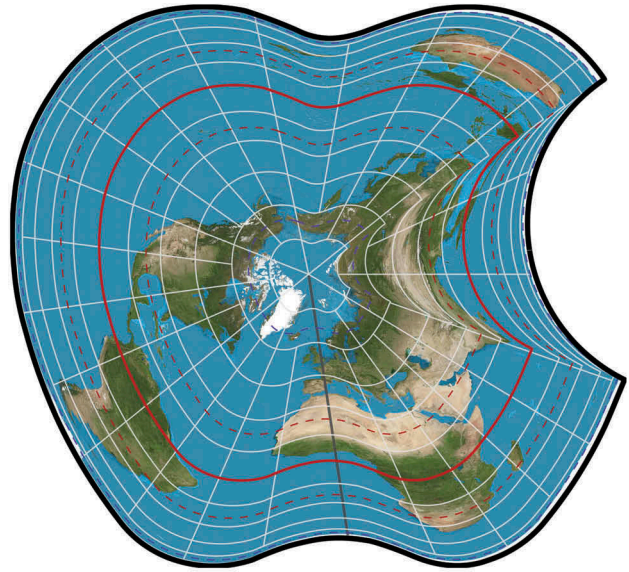


**Figure 11.** “Quasi-azimuthal equal-area apple” projection,  $15^\circ$  graticule,  $10^\circ$  increments in angular deformation (one-column).

equal-area projection in some particular shape, such as an ellipse or a square or an apple, is not unique. Qualifying the description with “quasi-azimuthal” specifies which among an unlimited number of projections it is.

Lastly, we observe that a plane-to-plane form of the equal-area condition in polar coordinates satisfies

$$\rho' \left( \frac{\partial \theta'}{\partial \theta} \frac{\partial \rho'}{\partial \rho} - \frac{\partial \theta'}{\partial \rho} \frac{\partial \rho'}{\partial \theta} \right) = \rho \quad (2.37)$$

where the primes mean the transformed coordinates, and without primes mean the original polar coordinates on the plane. We are no longer concerned with the original manifold; insofar as it got projected by some

equivalent means onto the plane, we can set our origin wherever we like and use Equation (2.37) to establish that the result truly preserves areas. As applied to planar radial oozing, we prohibit a dependency of  $\theta'$  on  $\rho$ , simplifying the condition to

$$\rho' \frac{\partial \theta'}{\partial \theta} \frac{\partial \rho'}{\partial \rho} = \rho. \quad (2.38)$$

As in the spherical case, we posit some function  $h(\theta)$  or  $h(\theta')$  to warp  $\rho$  into  $\rho'$ . We are no longer concerned about the spacing of parallels; this is merely linearly stretching  $\rho$  into  $\rho'$ , and so  $\rho' = h\rho$  and  $\partial \rho' / \partial \rho = h$ , and Equation (2.38) simplifies to

$$h^2(\theta) \frac{\partial \theta'}{\partial \theta} = 1 \quad \text{or} \quad h^2(\theta') \frac{\partial \theta'}{\partial \theta} = 1$$

and therefore

$$\frac{\partial \theta'}{\partial \theta} = h^{-2}(\theta) \quad \text{or} \quad \frac{\partial \theta'}{\partial \theta} = h^{-2}(\theta')$$

$$\theta' = \int \frac{d\theta}{h^2(\theta)} \quad \text{or} \quad \theta = \int h^2(\theta') d\theta'.$$

Applying this to the example of equivalently and radially oozing a unit circle into a square with sides of length  $\sqrt{\pi}$ , we have

$$\begin{aligned} h(\theta') &= \sqrt{\frac{\pi}{4}} \sec \theta', \quad \text{so} \\ \theta &= \frac{\pi}{4} \int \sec^2 \theta' d\theta' \\ &= \frac{\pi}{4} \tan \theta', \quad \text{and} \\ \theta' &= \arctan \frac{4\theta}{\pi} \\ \rho' &= \frac{\sqrt{\pi}}{2} \rho \sec \theta. \end{aligned} \quad (2.39)$$

And finally, I note that radial oozing is analogous to axial yanking. In radial oozing, the angle subtending meridians is specified by formula, just as is the linear spacing along the axis caused by yanking. The radial scaling is thereby determined by the derivative of the radial formulation, just as the perpendicular scaling is determined by the derivative of the axial yank.

### 3. Conclusion

I have gathered and described here 11 distinct methods for generating equal-area map projections. Three methods are new to the literature: axial yanking, directional

path offset, and radial oozing. I have identified the Bonne projection methodology as a transform in its own right. I have described novel uses for affine transformation, a method which seems not to have literature devoted to it in its most general forms. I have reported several novel projections as examples of using these techniques, and described the methods behind some projections found in the Geocart software but never described formally. Further, I proposed a way that affine transformation could be used to render locally correct maps for any region without having to re-render the underlying raster tiles based on a single projection. This technique would open up Web mapping to the use of any projection without discarding the benefits of the ubiquitous Web Mercator.

By consolidating these methods into one monograph, I hope to help map projection designers develop and explore the domain of equal-area projections. I find the theory of equivalent projections lacking when compared to conformal projection theory. As a description of techniques, the present work does not directly advance theory, but I nevertheless hope it will inspire ideas and research directed toward a comprehensive understanding of area-preserving transforms.

### Acknowledgments

I am grateful for the attention given to this paper by the several anonymous reviewers, as well as by my less anonymous wife, Tiffany Lillie. It is a better paper for their efforts.

### Disclosure statement

No potential conflict of interest was reported by the author.

### ORCID

Daniel “daan” Strebe  <http://orcid.org/0000-0001-6410-6259>

### References

- Abramms, B. (2006). *Background on Hobo-Dyer map*. Retrieved from [http://odtmaps.com/behind\\_the\\_maps/hobo-Dyer\\_map/default.asp](http://odtmaps.com/behind_the_maps/hobo-Dyer_map/default.asp)
- Aitoff, D. A. (1892). Note sur la projection zenithale equidistante et sur les canevas qui en est dérivé. *Nouvelles Géographiques*, 6, 87–90.
- Balthasart, M. (1935). L'emploi de la projection cylindrique équivalente dans l'enseignement de la géographie. *Société Belge d'Études Géographiques*, 5, 269–272.
- Battersby, S. E., Finn, M. P., Usery, E. L., & Yamamoto, K. H. (2014). Implications of Web Mercator and its use in online mapping. *Cartographica: The International Journal for*

- Geographic Information and Geovisualization*, 49, 85–101. doi:10.3138/carto.49.2.2313.
- Battersby, S. E., Strebe, D., & Finn, M. P. (2017). Shapes on a plane: Evaluating the impact of projection distortion on spatial binning. *Cartography and Geographic Information Science*, 44, 410–421. doi:10.1080/15230406.2016.1180263
- Behrmann, W. (1910). Die beste bekannte flächentreue Projektion der ganzen Erde. *Petermanns Geographische Mitteilungen*, 56(part 2), 141–144.
- Boggs, S. W. (1929). A new equal-area projection for world maps. *The Geographical Journal*, 73, 241–245. doi:10.2307/1784714
- Böhm, R. (2006). Variationen von Weltkartennetzen der Wagner-Hammer-Aitoff-Entwurfamilie. *Kartographische Nachrichten*, 56, 8–16.
- Canter, F. (2002). *Small-scale map projection design*. London: Taylor & Francis.
- Craster, J. (1929). Some equal-area projections of the sphere. *The Geographical Journal*, 74, 471–474. doi:10.2307/1783643
- Dominguez, J. (2016). *Tableau maps tricks and tips*. Retrieved from <https://community.tableau.com/community/support-blog/blog/2016/01/14/tableau-maps-tips-and-tricks-by-jared-dominguez>.
- Dyer, J. A., & Snyder, J. P. (1989). Minimum-error equal-area map projections. *The American Cartographer*, 16, 39–46. doi:10.1559/152304089783875613.
- Edwards, T. (1953). *A new map of the world*. London: B.T. Batsford.
- Gall, J. (1885). Use of cylindrical projections for geographical, astronomical, and scientific purposes. *Scottish Geographical Magazine*, 1, 119–123. doi:10.1080/14702548508553829
- Gartner Inc. (2017). *Magic quadrant for business intelligence and analytics platforms*. Retrieved from <https://www.gartner.com/doc/3611117/magic-quadrant-business-intelligence-analytics>
- Hammer, E. (1892). Über die Planisphäre von Aitow und verwandte Entwürfe, insbesondere neue flächentreue ähnlicher Art. *Petermanns Mitteilungen*, 38, 85–87.
- Jenny, B. (2012). Adaptive composite map projections. *IEEE Transactions on Visualization & Computer Graphics*, 18, 2575–2582. doi:10.1109/TVCG.2012.192
- Jenny, B., & Šavrič, B. (2017). Enhancing adaptive composite map projections: Wagner transformation between the Lambert azimuthal and the transverse cylindrical equal-area projections. *Cartography and Geographic Information Science*, 1–8. doi:10.1080/15230406.2017.1379036
- Kronenfeld, B. (2010). Sphere-to-sphere projections: Proportional enlargement on a spherical surface. *Cartographica: the International Journal for Geographic Information and Geovisualization*, 45, 152–158. doi:10.3138/carto.45.2.152
- Laskowski, P. H. (1989). The traditional and modern look at Tissot's indicatrix. *The American Cartographer*, 16, 123–133. doi:10.1559/152304089783875497
- Mapbox. (2017). *Vector tiles*. Retrieved from <https://www.mapbox.com/vector-tiles/>
- Muñoz, A. (2015). Maps: About Mercator projection. Retrieved from <https://community.qlik.com/blogs/qlikview/designblog/2015/01/09/what-you-see-may-not-be-true>
- New York Times. (2011). Science, skin and ink. *New York Times*, Slide 17. Retrieved from <http://www.nytimes.com/slideshow/2011/11/07/science/20111107-tattoos-17.html>
- Peters, A. (1983). *The new cartography*. New York: The Friendship Press.
- Raposo, P. (2013). Interview with a celebrity cartographer: Daniel (daan) Strebe. *Cartographic Perspectives*, 75, 63–66. <http://cartographicperspectives.org/index.php/journal/article/view/cp75-raposo-strebe/1288>
- Rasmussen, J., Rasmussen, L., & Ma, S. (2011). *Generating and serving tiles in a digital mapping system*. US Patent 7,962,281.
- Šavrič, B., & Jenny, B. (2014). A new pseudocylindrical equal-area projection for adaptive composite map projections. *International Journal of Geographical Information Science*, 28, 2373–2389. doi:10.1080/13658816.2014.924628
- Šavrič, B., Jenny, B., White, D., & Strebe, D. R. (2015). User preferences for world map projections. *Cartography and Geographic Information Science*, 42, 398–409. doi:10.1080/15230406.2015.1014425
- Smyth, C. P. (1870). *On an equal-surface projection for maps of the world, and its application to certain anthropological questions*. Edinburgh: Edmonston & Douglas.
- Snyder, J. P. (1985). *Computer-assisted map projection research* (Bulletin 1629). Washington, DC: US Geological Survey. Retrieved from <https://pubs.usgs.gov/bul/1629/report.pdf>
- Snyder, J. P. (1989). *An album of map projections* (Professional Paper 1453). Washington, DC: US Geological Survey. Retrieved from <https://pubs.usgs.gov/pp/1453/report.pdf>
- Snyder, J. P. (1992). An equal-area map projection for polyhedral globes. *Cartographica: the International Journal for Geographic Information and Geovisualization*, 29, 10–21. doi:10.3138/27H7-8K88-4882-1752
- Snyder, J. P. (1993). *Flattening the Earth: Two thousand years of map projections*. Chicago: University of Chicago Press.
- Sørensen, H. (2012). High-performance matrix-vector multiplication on the GPU. In M. Alexander, et al., (Eds.). *Euro-Par 2011: Parallel processing workshops, part I* (pp. 377–386). Berlin: Springer. doi:10.1007/978-3-642-29737-3\_42
- Strebe, D. (1992). *Geocart 1.2*. Croton-on-Hudson, NY: Terra Data, Inc.
- Strebe, D. (1994). *Geocart 2.0*. Croton-on-Hudson, NY: Terra Data, Inc.
- Strebe, D. (2016). An adaptable equal-area pseudoconic map projection. *Cartography and Geographic Information Science*, 43, 338–345. doi:10.1080/15230406.2015.1088800
- Strebe, D. (2017). An efficient technique for creating a continuum of equal-area map projections. *Cartography and Geographic Information Science*. doi:10.1080/15230406.2017.1405285
- Strebe, D. (2018). *Geocart 3.2*. Seattle, WA: Maphematics LLC.
- Strebe, D., Gamache, M., Vessels, J., & Tóth, T. (2012). Mapping the oceans. *National Geographic Magazine*, Digital Edition 9. Retrieved from <https://www.youtube.com/watch?v=OQCoWAbOKfg>
- Tissot, N. A. (1881). *Mémoire sur la représentation des surfaces et les projections des cartes géographiques*. Paris: Gauthier-Villars.
- Tobler, W. R. (1972). *Notes and comments on the composition of terrestrial and celestial maps by J.H. Lambert*. Ann Arbor: University of Michigan. 2011 edition available from ESRI Press.
- Tobler, W. R. (2008). Unusual map projections. *Cartographic Perspectives*, 59, 28–40. doi: 10.14714/CP59.246



- Tobler, W. R., & Chen, Z. (1986). A quadtree for global information storage. *Geographical Analysis*, 18, 360–371. doi:10.1111/j.1538-4632.1986.tb00108.x
- US NGA Office of Geomatics. (2014). *Implementation Practice: Web Mercator Map Projection* (Standardization Document NGA.SIG.0011 1.0.0 WEBMERC). Springfield, VA: National Geospatial-Intelligence Agency.
- Van Leeuwen, D., & Strebe, D. (2006). A “slice-and-dice” approach to area equivalence in polyhedral map projections. *Cartography and Geographic Information Science*, 33, 269–286. doi: 10.1559/152304006779500687
- Wagner, K. (1932). Die unechten Zylinderprojektionen. *Aus dem Archiv der Deutschen Seewarte*, 51, 68.
- Zimmer, C. (2011). *Science ink*. New York: Sterling.